Conformational stability, vibrational assignmenents, barriers to internal rotations and ab initio calculations of 2-aminophenol (do and d3)

ARTICLE *in* SPECTROCHIMICA ACTA PART A MOLECULAR AND BIOMOLECULAR SPECTROSCOPY · DECEMBER 2007

Impact Factor: 2.35 · DOI: 10.1016/j.saa.2006.12.047 · Source: PubMed

3 AUTHORS:

Usama Soliman
Al-Azhar University
11 PUBLICATIONS **32** CITATIONS
SEE PROFILE

Ali M. A. Hassan
Al-Azhar University
43 PUBLICATIONS **147** CITATIONS
SEE PROFILE

Tarek Mohamed
Al-Azhar University
48 PUBLICATIONS **373** CITATIONS
SEE PROFILE

Available online at www.sciencedirect.com
ScienceDirect
Spectrochimica Acta Part A 68 (2007) 688–700
SPECTROCHIMICA ACTA PART A
www.elsevier.com/locate/saa

Conformational stability, vibrational assignmenents, barriers to internal rotations and *ab initio* calculations of 2-aminophenol (d_0 and d_3)

Usama A. Soliman [1], Ali M. Hassan, Tarek A. Mohamed *

Department of Chemistry, Faculty of Science (Boys), Al-Azhar University, Nasr City 11884, Cairo, Egypt

Received 8 November 2006; received in revised form 26 December 2006; accepted 31 December 2006

Abstract

The Raman (3700–100 cm^{-1}) and infrared (4000–400 cm^{-1}) spectra of solid 2-aminophenol (2AP) have been recorded. The internal rotation of both OH and NH_2 moieties produce ten conformers with either C_s or C_1 symmetry. However, the calculated energies as well as the imaginary vibrational frequencies reduce rotational isomerism to five isomers. The molecular geometry has been optimized without any constraints using RHF, MP2 and B3LYP levels of theory at 6-31G(d), 6–311+G(d) and 6–31++G(d,p) basis sets. All calculations predict **1** (*cis*; OH is directed towards NH_2) to be the most stable conformation except RHF/6–31++G(d,p) basis set. The **1** (*cis*) isomer is found to be more stable than **8** (*trans*; OH is away from the NH_2 moiety and the NH bonds are out-of-plane) by 1.7 kcal/mol (598 cm^{-1}) as obtained from MP2/6-31G(d) calculations. Aided by experimental and theoretical vibrational spectra, *cis* and *trans* 2AP are coexist in solution but *cis* isomer is more likely present in the crystalline state. Aided by MP2 and B3LYP frequency calculations, molecular force fields, simulated vibrational spectra utilizing 6-31G(d) basis set as well as normal coordinate analysis, complete vibrational assignments for $HOC_6H_4NH_2$ and $DOC_6H_4ND_2$ have been proposed. Furthermore, we carried out potential surface scan, to determine the barriers to internal rotations of NH_2 and OH groups. All results are reported herein and compared with similar molecules when appropriate.

Keywords: 2-Aminophenol; Raman spectrum; Vibrational assignments; Barriers to internal rotations; *Ab initio* calculations

1. Introduction

Aminophenols (APs) are attention-grabbing electrochemical materials, they could show electrochemical behavior resembling anilines [1,2] and/or phenols [3]. In addition, APs are used as intermediates for photographic, pharmaceutical, chemical dye industries [4,5], thin polymeric films and polymer-modified electrodes [6,7]. Additionally, their thermodynamic properties play an important task in biological applications [8]. The vibrational spectra (IR, R, SERS) of aniline, *o*-, *m*-, and *p*-substituted anilines have been subject of several investigations [9–18]. The conformational stability and vibrational assignments of 2-aminophenols [14,15], and its complexes [15,16] along with 3-aminophenol [16,19] were in favor of *cis* and *trans* isomers. Moreover, theoretical AM1 [20] and *ab* initio calculations were carried out to study the thermodynamic properties of 2-aminophenol [21], 3-aminophenol [22], and 4-aminophenol [23,24]. Although the crystal structure of 2AP has been reported [25], the hydrogen atoms of the π-electron donor groups OH and NH_2 could not be located. In fact, the position of hydrogen atom is the dominant factor in the conformational interchange of 2AP.

In earlier investigations [14,15,19,21], all hypothetical rotational isomerism of APs in general and 2AP in particular assuming NH_2 (SP^3), NH_2 planar (SP^2), OH in-plane and/or out-of-plane are not considered yet. To the best of our knowledge, neither normal coordinate analysis (NCA), nor the barriers to internal rotation of 2AP have been reported, as yet. Therefore, we have carried out Gaussian 98 [26] *ab initio* calculations [27] supported by NCA utilizing the 6-31G(d) basis set at the levels of MP2 and B3LYP [27–33] to determine the optimized structural parameters (SPs), harmonic force constants (FCs), vibrational frequencies, infrared intensities and Raman activities. To determine the barriers to internal rotations around C–O and C–N, we have also employed potential surface scan (PSS) for both OH and NH_2 moieties, respectively. The results are reported herein and compared to similar molecules whenever appropriate.

* Corresponding author. Tel.: +202 7200773; fax: +202 2629356.
E-mail address: tarekama@hotmail.com (T.A. Mohamed).
[1] Taken in part from the Master Thesis of U.A. Soliman which will be submitted to Chemistry Department, Faculty of Science (Boys), Al Azhar University, Nasr City, Cairo 11884, Egypt.

1386-1425/$ – see front matter © 2007 Elsevier B.V. All rights reserved.
doi:10.1016/j.saa.2006.12.047

2. Experimental

The sample of 2-aminophenol ($HOC_6H_4NH_2$), 99% grade was obtained from Aldrich Chemical Company, Egypt branch and has been used without further purification. The solid sample is finely grounded in agate mortar before recording the Raman spectrum of the solid (R_S) to minimize fluorescence. The Raman spectra (Fig. 1) were recorded with a Nexus-670- Nicolet Fourier Transform Raman spectrometer in the range of 3700–100 cm^{-1}. The spectrophotometer is equipped with 1064 nm radiation from a Nd:YAG laser and an output of ~0.48–0.5 W was used for excitation while collecting 64 scans. The Raman (R) spectrum was measured using FT-R accessories at the National Research Institute, Dokki, Cairo, Egypt. The solid sample is prepared using KBr disc technique and the mid-infrared solid spectrum (IR_S) is recorded on Fourier-Transform Perkin-Elmer (spectrum RX) at the Chemistry, Department, Faculty of Science, Al-Azhar University. Forty scans at 4 cm^{-1} resolution were collected in the region of 4000–400 cm^{-1} (Fig. 2). The observed R and IR spectral data of 2AP are summarized in Tables 1 and 2 and compared to those reported for 2AP-d_0 ($HOC_6H_4NH_2$) and 2AP-d_3 ($DOC_6H_4ND_2$) [14] as well as the web (http://www.aist.go.jp/RIODB/SDBS).

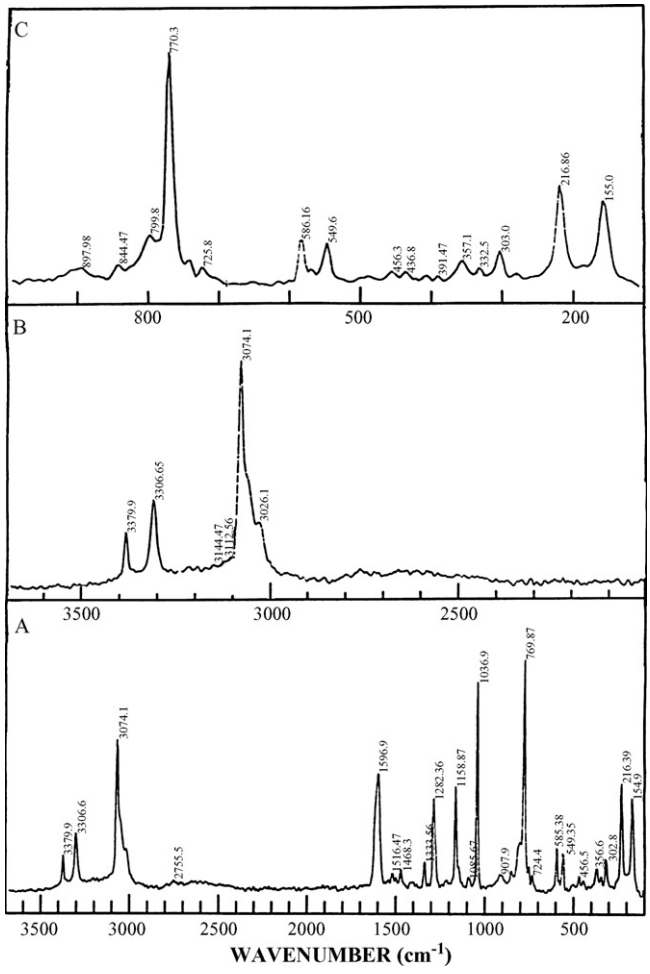

Fig. 1. Raman spectrum of solid 2-aminophenol; (A) from 100 to 3700 cm^{-1}; (B) expanded spectrum from 2500 to 3700 cm^{-1}; (C) expanded spectrum from 100 to 1000 cm^{-1}.

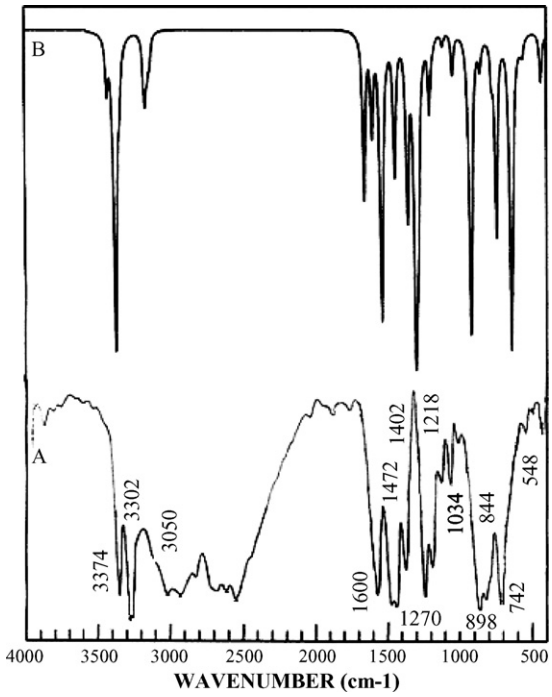

Fig. 2. The infrared spectrum of solid 2-aminophenol; top (calculated IR spectrum at MP2/6-31G(d) basis set); bottom (experimental from 400 to 4000 cm^{-1}).

3. Rotational isomerism

The OH group could be directed towards and away from NH_2 to yield **1** and **6** isomers, respectively (Figs. 3 and 4). Upon rotating the NH_2 moiety of *cis* (**1**) by C_6, C_3, C_2 and C_n ($0 < n < 60$) around the C–N bond, extra four isomers (**2**, **3**, **4** and **5**) are obtained. Similarly, isomers **7**, **8** (*trans*), **9** and **10** are revealed when rotating NH_2 of **6** conformer. To maintain C_s symmetry of conformers **1** and **6**, all atoms are kept in plane except the two N–H bonds. Furthermore, the hydroxyl group could be out of plane of benzene ring which doubles the number of theoretical isomerism. Moreover, an extra conformer (**11**) has been considered where the hydroxyl group is perpendicular (⊥) to benzene ring. On the other hand, an increase of C–N bond length causes SP^3 hybridization for NH_2 but the shortening of C–N bond represents SP^2 type [25], thus, two extra planar conformers **12** and **13** are also proposed, supplement A. Initially, the SPs are obtained using semi-empirical calculations [34] using CAChe 3.2 program [35]. Consequently, we have carried out quantum mechanical (QM) calculations [27,28], where the energy minima with respect to the nuclear coordinates have been obtained by simultaneous relaxation of all geometrical parameters by using the gradient method of Pulay [36].

Only five conformers are fully converged (**1**, **2**, **7**, **8** and **9**) with real frequencies with *cis* **1** is the least energy conformer, the energy differences (ΔE, cm^{-1}) between each isomer and the most stable **1** (*cis*) are given in Figs. 3 and 4. When optimizing

Table 1
Observed[a] and calculated wavenumbers and potential energy distributions for *cis* 2-aminophenol (-d_0 and -d_3)

No.	Fundamental	*ortho*-$HOC_4H_6NH_2$									*ortho*-$DOC_4H_6ND_2$				
		Ab initio	Fixed scaled[b]	IR Int.[c]	R act.[d]	Observed[e] Ref. [14]		This study		PED[f]	Ab initio	Fixed scaled[b]	Obs.[e] Ref. [14]		PED[f]
						IR_{liquid}	R_{liquid}	IR_S	R_S				IR_S	R_S	
ν_1	$\upsilon_{as}NH_2$ ND_2	3612	3426	13.3	77.6	3450s	*3376	3374vs	3380m	$100S_1$	2662	2526	2527s	2530(3)	$100S_1$
ν_2	υ_sOH	3552	3370	142.2	49.5	∼3400s	–	2962br	3026sh	$100S_2$	2583	2451	2185	–	$100S_2$
ν_3	$\upsilon_s NH_2$	3518	3338	13.6	166.0	3380s	3354w,p	3302vs	3307m	$99S_3$	2544	2414	2415	2414(2)	$99S_3$
ν_4	υ_sCH	3253	3171	5.8	176.8	*3080sh	3066(7),p	(3128sh)	3074s	$69S_4 20S_6 10S_7$	3253	3171	3058m	3068(10)	$69S_4 20S_6 10S_7$
ν_5	υ_sCH	3245	3162	14.7	86.0	–	3048(7),p	(3128sh)	3074s	$46S_5 36S_6 17S_4$	3245	3162	3058m	3068(10)	$46S_5 36S_6 17S_4$
ν_6	υ_sCH	3228	3146	7.3	71.4	*3051w	3048(7),p	(3050vs)	(3060sh)	$35S_6 41S_7 23S_5$	3227	3146	3030m	3038(2)	$40S_6 41S_7 23S_5$
ν_7	υ_sCH	3210	3129	7.09	65.9	*3021w	3048(7),p	(3050vs)	(3060sh)	$48S_7 29S_6 13S_4$	3210	3129	3030m	3016(1)	$48S_7 29S_6 14S_4$
ν_8	$\delta_{scissors}NH_2/ND_2$	1713	1654	49.8	21.4	1620s	1609(2),p	(1600vs)	(1597br)	$57S_8 18S_{22} 16S_{10}$	1214	1162	1200sh∼	–	$44S_8 14S_{22} 13S_{19}$
ν_9	Ring stretch	1692	1647	1.6	10.1	1610sh	1598(3)	(1600vs)	(1597br)	$43S_9 25S_{21}$	1687	1650	1592s	1599(4)	$40S_9 20S_{21} 11S_{10} 11S_{17}$
ν_{10}	Ring stretch	1659	1598	20.1	10.5	1590m	1592(2),dp	(1600vs)	(1597br)	$37S_{10} 22S_8 15S_{20}$	1665	1625	–	1593sh	$48S_{10} 15S_{20}$
ν_{11}	δCH in-plane	1562	1532	116.1	2.8	*1513s	1512w,p	1506ssh	1516w	$33S_{11} 21S_{21} 10S_{20} 10S_{15}$	1561	1530	1507s	1506(4)	$34S_{11} 20S_{21}$
ν_{12}	δCH in-plane	1531	1493	0.75	2.9	*1471sbr	1462w,p	1472vs	1468wbr	$34S_{12} 17S_{14} 13S_{20} 10S_{10}$	1520	1487	1452s	1455(w)	$45S_{12} 21S_{20}$
ν_{13}	Ring stretch	1483	1442	40.3	1.01	1395s	1380w	1402s	1410vw	$67S_{13} 15S_{14}$	1469	1431	1319w	1319(1)	$90S_{13}$
ν_{14}	δOH/OD in-plane	1397	1354	56.2	5.1	1340m	1338(1),p	1370s	1334m	$45S_{14} 19S_{13} 16S_{12} 13S_{17}$	1009	965	1016m		$82S_{14} 13S_{24}$
ν_{15}	υC—O	1321	1296	146.4	6.7	1280s	1282(1),p	(1270vs)	1282s	$33S_{15} 15S_{11} 14S_{27}$	1342	1322	1298sh	1300sh	$36S_{15} 15S_{17} 13S_{12} 12S_{27}$
ν_{16}	υC—N	1303	1280	51.5	1.3	*1268s	*1274(2)	(1270vs)	1265vw	$20S_{16} 29S_{17} 12S_{12}$	1268	1246	1279s	1282(1)	$17S_{16} 21S_8 18S_{17} 14S_{24}$
ν_{17}	δCH in-plane	1231	1201	19.7	4.9	1230sh	–	1218s	1220vw	$29S_{17} 17S_9 16S_{16} 11S_{14}$	1324	1297	1245m	1239w	$34S_{17} 16S_{16} 10S_8$
ν_{18}	$\delta_{twist}NH_2/ND_2$	1219	1159	0.005	2.5	–	1122(1)	(1144m)	1159s	$100S_{18}$	947	910	830m		$86S_{18} 10S_{37}$
ν_{19}	δCH in-plane	1208	1178	1.5	4.9	1155w	1154(1),p	(1144m)	(1159)s	$63S_{19} 23S_{11}$	1207	1177	1151m	1157(2)	$52S_{19} 25S_{11}$
ν_{20}	Ring stretch	1140	1113	2.8	2.7	*1085m	–	1080m	1086w	$23S_{20} 21S_{24} 21S_{12} 10S_{17}$	1158	1129	1117m	1117(1)	$14S_{20} 23S_{12} 20S_{17} 14S_{24} 10S_9$
ν_{21}	Ring stretch	1068	1043	10.8	14.5	*1031m	1034(8),p	1024w	1037vs	$22S_{21} 27S_{27} 23S_{11} 10S_9$	1072	1046	1038s	1038(3)	$15S_{21} 25S_{27} 24S_{11} 13S_9$
ν_{22}	$\delta_{wag}NH_2/ND_2$	918	918	128.1	1.7	925w	*892w	928sh	908w	$71S_{22} 19S_{18}$	722	721	748w	753(2)	$63S_{22} 14S_8$
ν_{23}	δ_{wag}CH	877	877	0.068	0.7	865sh	–	898vs	898wsh	$55S_{23} 12S_{28}$	872	871	–	887(1)	$46S_{23} 12S_{25} 12S_{28}$
ν_{24}	δCCC	872	855	6.3	0.3	855m	–		870vwsh	$32S_{24} 24S_{33} 14S_{16}$	864	848	848m		$31S_{24} 27S_{33} 15S_{15}$
ν_{25}	δ_{wag}CH	848	848	1.4	0.9	855m	*844	844vs	844w	$60S_{25} 19S_{26} 13S_{28} 11S_{23}$	848	848	830m	847w	$59S_{25} 20S_{26} 14S_{28} 11S_{23}$
ν_{26}	δ_{wag}CH	815	815	0.04	5.6	*802m	*800w	800sh	800sh	$41S_{26} 26S_{28} 15S_{25}$	814	814	–	–	$42S_{26} 27S_{28} 14S_{25}$
ν_{27}	Ring breathing	788	774	8.8	23.2	750s	770(10)p	800sh	770vs	$43S_{27} 17S_{16} 11S_{15}$	790	774	748w	753(2)	$34S_{27} 22S_{16}$
ν_{28}	δ_{wag}CH	742	742	66.2	1.3	740s	*742(1)	742vsbr	748sh	$36S_{28} 28S_{23} 20S_{36} 11S_{25}$	739	738	738w	–	$35S_{28} 29S_{23} 19S_{26} 10S_{25}$
ν_{29}	OH/OD torsion	734	550	141.9	3.4		487w			$82S_{29}$	546	467	442m?	–	$62S_{29} 13S_{22??}$
ν_{30}	δCCC	588	577	1.7	7.2	*581w	582(1),p		586m	$62S_{30} 12S_{31??}$	581	571	–	578(1)	$60S_{30} 10S_{31}$
ν_{31}	δ_{ring}CCC	567	562	4.2	4.3	*569w	569w		570sh	$38S_{31} 22S_{36} 16S_{24}$	418	415	437m	456w	$21S_{31} 24S_{23}$
ν_{32}	δ_{wag}C—O	534	534	0.2	0.002	*549m	564(1),p	548w	550m	$46S_{32} 13S_{35} 11S_{34}$	517	516	531m	531(1)	$33S_{32} 21S_{35} 12S_{37}$
ν_{33}	δ_{ring}CCC	439	436	12.0	0.9	*448m	460wbr		(437w)	$29S_{33} 24S_{36} 12S_{20}$	551	546	558m	559w	$40S_{33} 18S_{36} 16S_{24} 10S_{20}$
ν_{34}	Ring puckering	432	432	1.5	0.2	*422w	460wbr		(437w)	$37S_{34} 25S_{32} 13S_{38}$	428	428	442m	456w	$39S_{34} 26S_{32} 14S_{38}$
ν_{35}	Ring puckering	391	391	2.4	0.22	*361m	*354(1)		357wbr	$32S_{35} 34S_{37} 14S_{35} 11S_{39}$	387	387	–	–	$34S_{35} 30S_{28} 14S_{32} 11S_{39}$
ν_{36}	δCCN	336	334	5.8	0.5		*330w	333w,303w		$56S_{26} 11S_{30}$	306	304	–	308w	$29S_{36} 12S_{14} 10S_{30}$
ν_{37}	NH_2/ND_2torsion	265	245	4.6	2.7		*300w		279vw	$64S_{37} 20S_{35}$	254	245	–	278w	$60S_{37} 22S_{35}$
ν_{38}	Ring puckering	199	198	0.029	1.8		202(1),dp		217s	$17S_{38} 50S_{34} 17S_{35} 13S_{29}$	191	191	–	206(3)	$19S_{38} 54S_{34} 17S_{35} 13S_{37}$
ν_{39}	Ring puckering	67	67	19.3	2.5					$19S_{39} 28S_{38} 14S_{26} 13S_{28}$	49	49	–	–	$18S_{39} 26S_{38} 14S_{26}$

[a] Unscaled *ab initio* wavenumbers for *cis* 2-AP utilizing MP231G(d) basis set. Fundamentals from υ_{27} to υ_{39} belong to A'' species.

[b] Fixed scaled *ab initio* wavenumbers for *cis* 2-AP utilizing B3LYP/6-31G(d) basis set using scaling factors of 0.95 for υCH, υCC, δCH, δCC, δHCC and δHNH modes, 0.9 for υOH, υNH, δHOC and δHNC. But 1.0 scaling factor is used for υCN, υCO, δ_{wag}CN, δ_{wag}CO, $\delta_{wag}NH_2$, δNCC, δCCO and τCCCC and 0.75 for τOH and τNH_2.

[c] Calculated Raman activities in $^\circ A^4$/amu at MP2/6-31G(d) basis set.

[d] Calculated infrared intensities in kcal/mol at MP2/6-31G(d) basis set.

[e] Observed bands marked with asterisks are from IR and/or R spectra of the solid. Bands between brackets are used for two fundamentals modes.

[f] Contributions less than 10% are omitted.

Table 2
Observed[a] and calculated wavenumbers and potential energy distributions for *trans* 2-aminophenol ($HOC_6H_4NH_2$ and $DOC_6H_4ND_2$)

No.	Fundamental	*ortho*-$HOC_6H_4NH_2$							*ortho*-$DOC_6H_4ND_2$		
		Ab initio	scaled[b]	IR int.[c]	R act.[d]	Obs. [e] Ref. [14]		PED's[f]	Ab initio	Scaled[b]	PED's[f]
						$IR_{liq.}$	$R_{liq.}$				
ν_1	$\upsilon_{as}NH_2/ND_2$	3687	3498	21.9	52.5	3450s	–	$100S_1$	2723	2584	$100S_1$
ν_2	υ_sOH/OD	3763	3570	63.3	94.0	∼3400s	–	$100S_2$	2739	2599	$100S_2$
ν_3	υ_sNH_2/ND_2	3572	3389	24.6	140.8	3380s	3354w,p	$100S_3$	2582	2450	$100S_3$
ν_4	υ_sCH	3249	3167	14.1	184.6	–	3066(7),p	$68S_4 30S_5$	3249	3167	$68S_4 30S_5$
ν_5	υ_sCH	3213	3131	6.8	87.8	–	3048(7),p	$44S_5 35S_7 16S_4$	3213	3131	$44S_5 35S_7 16S_4$
ν_6	υ_sCH	3233	3152	10.8	59.9	–	3048(7),p	$79S_6 20S_7$	3233	3152	$79S_6 20S_7$
ν_7	υ_sCH	3201	3120	13.6	67.2	–	3048(7),p	$44S_7 25S_5 16S_6 14S_4$	3201	3120	$44S_7 26S_5 16S_6$, $14S_4$
ν_8	$\delta_{scissors}NH_2/ND_2$	1713	1664	87.4	26.7	1620s	1609(2),p	$40S_8 16S_{21} 16S_9 11S_{22}$	1202	1159	$28S_8 15S_{22} 10S_{12} 10S_{20}$
ν_9	Ring stretch	1678	1607	19.7	4.71	1590m	1592(2),dp?	$14S_9 31S_{10} 13S_8$	1691	1654	$42S_9 30S_{21}$
ν_{10}	Ring stretch	1686	1641	17.7	7.3	1610sh	1598(3)	$29S_{10} 19S_8 10S_9$	1672	1632	$61S_{10} 12S_{20}$
ν_{11}	δCH in-plane	1582	1549	103.5	2.7	–	1512w,p	$30S_{11} 16S_{21} 10S_{20}$	1577	1545	$31S_{11} 17S_{21} 12S_9$
ν_{12}	δCH in-plane	1527	1490	23.2	1.0		1462w,p	$38S_{12} 23S_{20}$	1519	1484	$42S_{12} 21S_{20}$
ν_{13}	Ring stretch	1498	1458	0.1	4.3	1395s	1380w	$81S_{13}$	1486	1448	$83S_{13}$
ν_{14}	δOH/OD in-plane	1385	1340	14.3	0.7	1340m	1338(1),p	$40S_{14} 38S_{17} 21S_{12} 12S_{18}$	954	911	$60S_{14}$
ν_{15}	υC—O	1299	1281	18.9	2.0	–	–	$31S_{15} 14S_{24} 10S_{16} 10S_{17}$	1290	1266	$31S_{15} 14S_{24} 13S_8$
ν_{16}	υC—N	1352	1329	124.0	11.6	1280s	1282(1),p	$37S_{16} 20S_{11} 16SS_{27} 10S_{15}$	1372	1346	$35SS_{16} 15S_8 15S_{11} 10S_{27}$
ν_{17}	δCH in-plane	1211	1173	58.8	5.2	1230sh	–	$18S_{17} 24S_{19} 12S_{11}$	1337	1309	$52S_{17} 13S_{12} 11S_{15}$
ν_{18}	$\delta_{twist}NH_2/ND_2$	1188	1140	80.4	2.7	1135m	1122(1)	$38S_{18} 10S_{20}$	913	879	$56S_{18} 15S_{24}$
ν_{19}	δCH in-plane	1214	1182	22.7	4.6	1155w	1154(1)	$39S_{19} 18S_{17} 12S_9 11S_{11}$	1213	1182	$59S_{19} 14S_{11}$
ν_{20}	Ring stretch	1075	1047	5.4	14.7	–	1034(8),p	$16S_{20} 26S_{27} 16S_{11} 12S_{21}$	1155	1123	$11S_{20} 22S_{24} 17S_{12} 13S_{17}$
ν_{21}	Ring stretch	1107	1074	19.4	1.4	–	–	$16S_{21} 23S_{24} 19S_{18} 11S_{12}$	1083	1058	$20S_{21,} 25S_{27} 22S_{11} 10S_9 10S_{20}$
ν_{22}	$\delta_{wag}NH_2/ND_2$	707	707	190.6	9.4	726sh?	724sh?	$40S_{22} 16S_8 12S_{26} 10S_{23} 10S_{25}$	589	589	$37S_{22} 20S_{37} 19S_8$
ν_{23}	δ_{wag}CH	811	811	3.1	2.2		–	$53S_{23} 33S_{26} 14S_{25} 13S_{28}$	811	811	$53S_{23} 34S_{26} 14S_{25} 14S_{28}$
ν_{24}	δCCC	877	859	27.1	1.1	(855wm)	–	$35S_{24} 26S_{33} 10S_{15}$	852	831	$17S_{24} 22S_{33} 11S_{18} 10S_{16} 10S_{25}$
ν_{25}	δ_{wag}CH	854	854	0.2	0.2	(855wm)		$60S_{25} 32S_{23}$	855	854	$51S_{25} 28S_{23}$
ν_{26}	δ_{wag}CH	730	725	2.6	0.7			$24S_{26} 20S_{22} 19S_{25}$	723	723	$35S_{26} 29S_{25} 18S_{23} 13S_{28}$
ν_{27}	Ring breathing	790	779	26.5	0.1	750s	770(10),p	$48S_{27} 17S_{15}$	762	745	$35S_{27} 12S_{16} 11S_{15} 10S_{21}$
ν_{28}	δ_{wag}CH	778	773	6.6	0.6	740s	770(10),p	$68S_{28} 21S_{26}$	778	777	$71S_{28} 20S_{26}$
ν_{29}	OH/OD torsion	331	327	19.9	0.2			$15S_{29} 26S_{37}$	210	185	$75S_{29}$
ν_{30}	δCCC	323	320	17.0	0.6			$15S_{30} 60S_{36}$	586	570	$54S_{30} 10S_{31} 10S_{22}$
ν_{31}	δ_{ring}CCC	594	583	1.6	6.8		582(1),p	$12S_{31} 64S_{30}$	415	412	$25S_{32} 22S_{36} 17S_{33}$
ν_{32}	δ_{wag}C—O	535	534	8.3	0.6		564(1),p	$37S_{32} 33S_{37}$	516	509	$41S_{31} 17S_{22} 15S_{37}$
ν_{33}	δ_{ring}CCC	547	543	3.8	2.7		564(1),p	$34S_{33} 17S_{36} 18S_{24}$	532	527	$43S_{33} 21S_{24} 12S_{36}$
ν_{34}	Ring puckering	283	247	81.8	3.6			$14S_{34} 53S_{29} 13S_{36}$	285	283	$50S_{34} 20S_{31} 16S_{37}$
ν_{35}	Ring puckering	305	293	19.0	1.5			$17S_{35} 52S_{342} 18S_{34} 14S_{29}$	419	418	$24S_{35} 16S_{37} 13S_{32} 10S_{36}$
ν_{36}	δCCN	443	441	3.3	0.8		460wbr	$33S_{36} 29S_{33} 14S_{20}$	295	294	$75S_{36} 13S_{30}$
ν_{37}	NH_2 torsion/ND_2	425	400	9.6	0.3			$24S_{37} 22S_{32} 50S_{38}$	321	297	$29S_{37} 31S_{32} 20S_{34}$
ν_{38}	Ring puckering	266	241	48.5	1.1		202(1),dp	$27S_{38,} 32S_{37} 18S_{29}$	206	177	$41S_{38} 16S_{29} 10S_{37} 10S_{35}$
ν_{39}	Ring puckering	173	172	1.3	1.7			$61S_{39}$	166	164	$60S_{39}$

[a] Observed bands for $-d_0$ 2AP ($HOC_6H_4NH_2$).

[b] Fixed scaled wavenumbers at MP2/6-31G(d) basis set using scaling factors of 0.97 for OH stretch, 0.95 for CH, NH and CC, stretches, HCC, HNH bending modes, 0.9 for HOC and HNC bending modes. And 1.0 scaling factor is used for υCN, υCO, δ_{wag}CH, δ_{wag}CN, $\delta_{wag}NH_2$, and δ_{wag}CO, τCCCC and 0.75 for τOH and τNH_2.

[c] Calculated Raman activities in $Å^4$/amu at MP2/6-31G(d) basis set.

[d] Calculated infrared intensities in kcal/mol at MP2/6-31G(d) basis set.

[e] Due to coincidence and overlapping in the calculated wavenumbers, single band could be interpreted for two or three fundamentals.

[f] Contributions less than 10% are omitted.

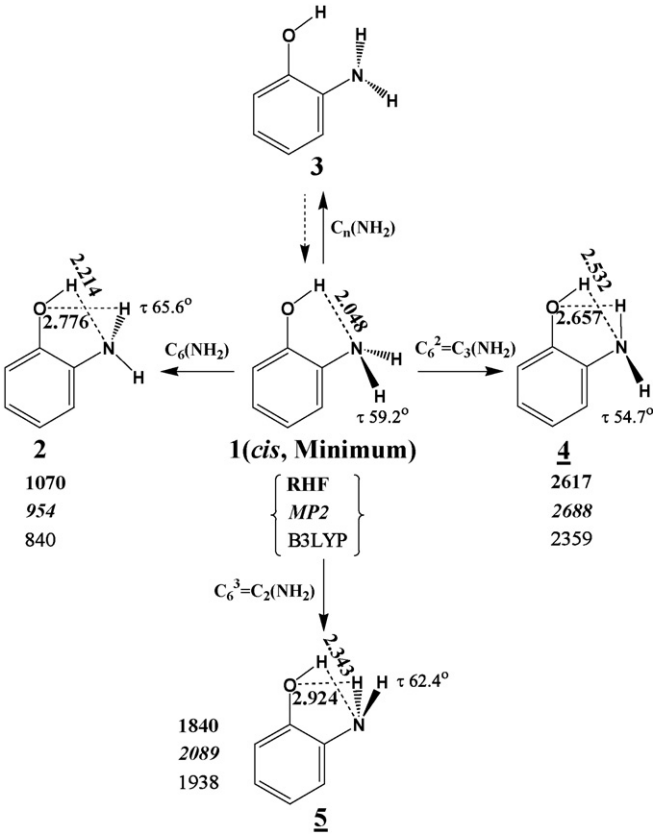

Fig. 3. Conformational isomerism of 2-aminophenol, where the OH group is directed towards the NH_2 moiety, the energy differences (ΔE) between all isomers and **1** (*cis*) is given in cm^{-1}.

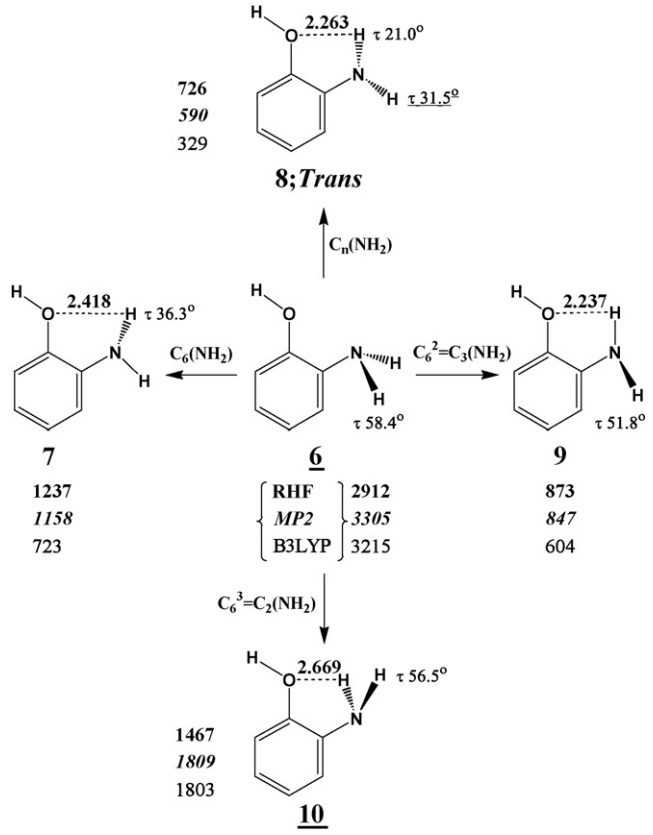

Fig. 4. Conformational isomerisms of 2-aminophenol, where the OH group is directed away from the NH_2 moiety, the energy differences (ΔE) between all isomers and **1** (*cis*) is given in cm^{-1}.

conformer **3** where the two NH bonds and lone-pair electron of nitrogen are out-of-plane, surprisingly it is converged to the least energy **1** (*cis*) rotamer (**3** → **1**). Additionally, for **8** isomer named *trans* (the NH bonds and the lone pair electrons are out-of-plane), the dihedral angles τC_5C_3NH and τC_1C_3NH are calculated at 31.5° and 21°, respectively, with **1** (*cis*) more stable than **8** (*trans*) by 590 cm^{-1}.

In order to account for lone pair interaction we have added the diffusion function to all levels of calculations and all results in favor of *cis* (**1**). It is very interesting that, ΔE between the *cis* and *trans* conformers (Table 3) decrease drastically in comparative levels and basis sets. On the other hand, the *trans* **8** isomer is predicted to be more stable than *cis* **1** by 101 cm^{-1} at RHF/6-31++G(d,p). The current calculations are consistent

Table 3
RHF, MP2 and B3LYP energies in Hartrees for 1, 8 and 9 conformations of 2-aminophenol molecule

	Cis; **1**	*Trans*; **8**	*Gauche*; **9**	ΔE_1[b] (cm^{-1})	ΔE_2[c] (cm^{-1})
At 6-31G(d) basis set					
RHF level	−360.5874447	−360.5841378	−360.583474	725	872
MP2 level	−361.6866096	−361.6839214	−361.6827508	590	847
B3LYP level	−362.818718	−362.8172786	−362.8159639	329	604
At 6-311+G(d) basis set					
RHF level	−360.6689589	−360.666415	−360.6656363	558	729
MP2[a] level	−361.9896921	−361.9886208	−361.9872512	235	536
B3LYP level	−362.9152725	−362.9147881	−362.9137293	106	339
At 6-31++G(d,p) basis set					
RHF level	−360.6188612	−360.6193227	−360.6185144	101[d]	76
MP2[a] level	−361.8142298	−361.8129757	−361.8117632	275	541
B3LYP level	−362.8567395	−362.8565771	−362.8556074	36	248

[a] Calculation's has been carried out with full electron correlation.
[b] ΔE_1 represents the energy difference between *cis* (the minimum energy, **1**) and *trans* isomer (**8**).
[c] ΔE_2 represents the energy difference between *cis* (the minimum energy, **1**) and *gauche* isomer (**9**).
[d] The *trans* isomer is more stable than *cis* by 101 cm^{-1}.

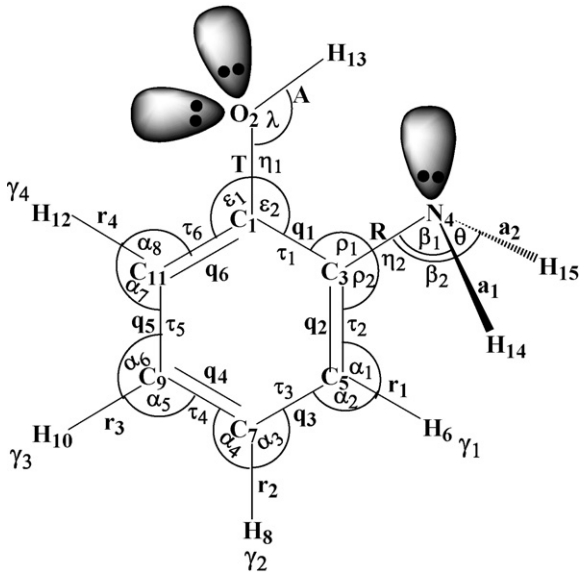

Fig. 5. Internal coordinates definitions of 2-aminophenol.

with standard enthalpies of formation [21] where *cis* (**1**) was found to be the most stable only if no diffuse functions are considered in the description of the atomic density. Alternatively, a reverse effect was observed in favour of **8** (*trans*) conformer upon introducing one extra diffuse function [21].

The underlined structures in Figs. 3 and 4 and supplement A indicate the prediction of at least an imaginary frequency. Hence, conformers **4**, **5**, **6**, **10** and **12** have been excluded, they are considered transition states. Furthermore, two imaginary wavenumbers were calculated for **11** and **13**, where ΔE of $\sim$4419 cm^{-1} has been obtained between **1** and **11** isomers. The MP2 optimized SPs, rotational constants and dipole moments (μ_{tot}) for **1** (*cis*) and **8** (*trans*) conformers up to 6-311++G(d,p) basis set are listed in Table 4. The B3LYP optimized geometries are also obtained for comparison purposes see supplement B and the calculated SPs, for *gauche* conformers (**2**, **7** and **9**) up to 6-31++G(d,p) basis set are available on request.

As indicated earlier, the OH group could be out-of-plane where τC_3C_1OH and $\tau C_{11}C_1OH$ larger than 0°, for atom numbering see Fig. 5. The optimized aforementioned torsion angles are ranged from 1° to 2.5° which did not allow significant changes in their optimized SPs, energies and frequencies among those given in Figs. 3 and 4. For instance, the calculated energies for **7** and **8** conformers vary only by 2–10 cm^{-1} and $\tau C_{11}C_1OH$ is $\sim$2–2.4°. Eventually, all computational calculations were carried out using Toshiba laptop (1.7 GHz), and/or Acer (2.93 GHz), 512 MB memory while the proposed structures of 2AP were visualized and confirmed using an interactive shareware molecular graphics program called MOLEKEL 4.0 [37].

4. Normal coordinate analysis

To carry out normal coordinate analysis (NCA), a similar method to symmetry adopted linear combination [38] have been implemented to describe the vibrational motion of 2AP. Local C_{3v} symmetry was chosen for benzene ring regarding the C–C ring stretching modes and C_{2v} symmetry for the CH stretches, while the molecule retains either C_s or C_1 symmetry. The vibrational modes span the irreducible representation to $26A'$ polarized bands and $13A''$ depolarized bands (C_s). Nevertheless polarized $39A'$ fundamentals are expected for C_1 *gauche* isomer. For C_s and C_1 point group, both A' and A'' species are IR and R active. Thus, 45 independent internal coordinates (Fig. 5) have been used to form 39 symmetry coordinates (Table 5) using the traditional method of Wilson [39].

The following procedure has been used to transform *ab initio* FCs into those required for iterative normal coordinate program. The Cartesian coordinates were input into G-matrix program, where the obtained B-matrix has been used to convert the unscaled *ab initio* force fields in Cartesian coordinates to that in chosen internal coordinates. The resultant force fields in internal coordinates for *cis* and *trans* compared with those reported earlier [16,19,40] are given in Table 6. All the diagonal elements of FCs have been assigned scaling factors into a force constant program similar to that written by Schachtschneider [41]. Initially, all scaling factors (SFs) have been kept fixed at a value of 1.0 to produce the pure *ab initio* calculated frequencies. Then, rational SFs were used to obtain the fixed scaled quantum mechanical (QM) molecular force field to bring the theoretical frequencies in close vicinity to the experimental values [42,43]. SFs are considered crucial to account for systematic error such as the neglect of basis set defects and electron correlation. Consequently, SFs of 0.95 have been used for υCH, υCC, δCH, δCC, δHCC and δHNH modes, 0.9 for υOH, υNH, δHOC and δHNC. But 1.0 scaling factor is used for υCN, υCO, δ_{wag}CN, δ_{wag}CO, δNCC, δCCO, $\delta_{wag}NH_2$ and τCCCC (ring puckering). Either OH and/or NH_2 torsion mode will break the existing intramolecular hydrogen bonding [44]; for that reason SFs of 0.75 has been used for these fundamentals. The unscaled and scaled frequencies utilizing MP2/6-31G(d) basis set along with the potential energy distributions (PEDs) for *cis* and *trans* conformers are given together in Tables 1 and 2, respectively. Whereas The calculated wavenumbers, IR intensities and R activities using B3LYP/6-31G(d) basis set are listed in supplement C.

5. Simulated infrared and Raman spectra

It has been already established that, a clear prediction of Raman (R) and infrared (IR) spectra became essential in vibrational analysis of organic molecules which makes vibrational spectroscopy a more practical tool [45–49]. To assist vibrational assignments of *cis* and *trans* conformers of 2AP, the simulated R spectra was generated using the calculated Raman scattering activities and scaled frequencies from MP2 (Tables 1, 2 and Fig. 6) and B3LYP (supplement C and D) levels at 6-31G(d) basis set. The Raman scattering cross section is proportional to the Raman intensity which can be calculated from the scattering activities and the predicted frequencies for each normal mode [50–53]. Moreover, the simulated IR spectra of *cis* conformer were calculated based on IR intensities and dipole moment (DM) derivatives with respect to the Cartesian coordinates. The DM derivatives were taken from the *ab initio* calculations then transformed to the normal coordinates. A detailed description

Table 4
MP2 and X-ray[a] structural parameters for *cis* and *trans* 2-aminophenol utilizing 6-31G(d), 6-311+G(d) and 6-31++G(d,p) basis sets

Parameters	X-ray	MP2 for *cis*			MP2 for *trans*		
	Ref. [25]	6-31G(d)	6-311+G(d)	6-31++G(d,p)	6-31G(d)	6-311+G(d)	6-31++G(d,p)
$r(O_2H_{13})$		0.986	0.987	0.974	0.973	0.963	0.966
$r(N_4H_{14})$		1.019	1.020	1.014	1.014	1.009	1.009
$r(N_4H_{15})$		1.019	1.020	1.014	1.015	1.010	1.010
$r(C_1O_2)$[b]	1.378(7)	1.361	1.365	1.355	1.382	1.375	1.382
$r(C_3N_4)$	1.429(7)	1.445	1.442	1.441	1.400	1.396	1.398
$r(C_1C_3)$[b]	1.397(8)	1.406	1.405	1.406	1.408	1.407	1.405
$r(C_3C_5)$	1.382(8)	1.396	1.397	1.398	1.398	1.400	1.399
$r(C_5C_7)$	1.414(9)	1.396	1.397	1.398	1.397	1.398	1.397
$r(C_7C_9)$	1.389(9)	1.399	1.399	1.400	1.394	1.396	1.395
$r(r(C_9C_{11})$	1.385(9)	1.394	1.395	1.396	1.399	1.400	1.398
$r(C_{11}C_1)$	1.385(8)	1.397	1.396	1.398	1.392	1.393	1.392
$r(C_5H_6)$	1.057(6)	1.089	1.089	1.089	1.089	1.089	1.084
$r(C_7H_8)$	1.055(7)	1.087	1.087	1.086	1.087	1.086	1.082
$r(C_9H_{10})$	1.149(7)	1.087	1.087	1.087	1.087	1.086	1.081
$r(C_{11}H_{12})$	1.105(6)	1.086	1.087	1.086	1.090	1.089	1.084
$r(O_2\cdots H_{14})$		3.394	3.394	3.386	3.606	3.613	3.615
$r(O_2\cdots H_{15})$		3.394	3.394	3.386	2.263[c]	2.276[c]	2.279[c]
$r(O_2\cdots H_{12})$		2.614[c]	2.612[c]	2.607[c]	2.703[c]	2.702[c]	2.699[c]
$r(N_4\cdots H_{13})$		2.048[c]	2.072[c]	2.084[c]	3.651	3.638	3.644
$\angle(C_1O_2H_{13})$		103.6	104.5	105.2	108.2	109.9	109.2
$\angle(O_2C_1C_{11})$	123.1(5)	120.0	119.7	119.8	123.6	123.7	123.6
$\angle(O_2C_1C_3)$	117.3(5)	119.8	119.9	119.9	115.3	115.3	115.3
$\angle(N_4C_3C_1)$	117.9(5)	114.9	115.1	115.1	119.3	119.4	119.4
$\angle(N_4C_3C_5)$	121.2(5)	125.3	125.3	125.2	122.5	122.5	122.4
$\angle(C_3C_1C_{11})$	119.6(5)	120.2	120.4	120.2	121.1	121.0	121.1
$\angle(C_1C_3C_5)$	120.5(5)	119.8	119.6	119.6	118.2	118.1	118.2
$\angle(C_3C_5C_7)$	119.5(6)	120.2	120.2	120.3	121.0	121.1	121.0
$\angle(C_5C_7C_9)$	119.7(6)	119.6	119.6	119.6	120.2	120.1	120.1
$\angle(C_7C_9C_{11})$	119.9(6)	120.7	120.7	120.6	119.5	119.5	119.5
$\angle(C_1C_{11}C_9)$	120.8(6)	119.5	119.4	119.6	120.0	120.1	120.0
$\angle(C_3N_4H_{14})$		110.7	111.6	111.6	113.3	114.2	114.2
$\angle(C_3N_4H_{15})$		110.7	111.6	111.6	112.6	113.7	113.8
$\angle(H_{14}N_4H_{15})$		106.9	107.6	108.0	111.3	112.3	112.1
$\angle(C_1C_{11}H_{12})$	122.9(6)	118.9	119.1	118.9	119.6	119.7	119.5
$\angle(C_9C_{11}H_{12})$	116.3(6)	121.6	121.5	121.5	120.4	120.2	120.4
$\angle(C_{11}C_9H_{10})$	121.3(6)	119.4	119.4	119.4	119.8	119.8	119.8
$\angle(C_7C_9H_{10})$	118.7(6)	119.9	119.9	120.0	120.7	120.7	120.7
$\angle(C_9C_7H_8)$	119.5(6)	120.3	120.3	120.4	120.3	120.3	120.3
$\angle(C_5C_7H_8)$	120.8(6)	120.1	120.0	120.1	119.6	119.6	119.6
$\angle(C_7C_5H_6)$	123.0(6)	120.5	120.5	120.5	120.2	120.0	120.2
$\angle(C_3C_5H_6)$	117.5(5)	119.3	119.3	119.2	118.8	118.8	118.8
$\tau C_1C_3N_4H_{15}$		120.8	119.8	119.6	21.0	20.7	20.5
$\tau C_1C_3N_4H_{14}$		120.8	119.8	119.6	−31.5	−28.6	−29.1
A (MHz)		3373	3370	3370	3350	3354	3352
B (MHz)		2205	2205	2205	2225	2224	2226
C (MHz)		1343	1342	1342	1339	1339	1340
μ_{tot} (Debye)		2.854	2.944	2.846	1.720	1.426	1.460

[a] Corrected X-ray structural parameters (distances in angstroms and angles in degrees).
[b] Uncorrected values for C_1O_2 and C_1C_3 distances are 1.368(7) and 1.418(7) Å [25], respectively.
[c] Intramolecular hydrogen bonding.

for entire procedure for calculating both R and IR vibrational spectra was given in Ref. [54]. Although there are some differences in the calculated versus experimental intensities, these data demonstrate the utility of *ab initio* calculations in predicting the spectrum to aid in vibrational assignments for 2AP. Moreover, the differences are undoubtedly devoted for two types of hydrogen bonding in the solid phase in agreement with X-ray crystallographic data [14,25].

6. Vibrational assignments and discussion

Earlier investigations of AP derivatives [12,14,19,21] neglect the hypothetical rotational isomerism (Figs. 3 and 4 and supplement A). They only assume *cis* (C_S) and *trans* (C_1) conformations, where none of N–H bonds eclipse benzene ring. In the current theoretical study, extra high energy *gauche* conformers with real frequencies were verified (**2**, **7** and **9**).

Table 5
Symmetry coordinates[a] for 2-aminophenol (-d_0 and -d_3) molecule

Species	ν_i[b]	Definition	Symmetry Coordinate
A''	ν_1	NH_2/ND_2 antisymmetric stretch.	$S_1 = a_1 - a_2$
A'	ν_2	OH/OD symmetric stretch	$S_2 = A$
A'	ν_3	NH_2/ND_2 symmetric stretch	$S_3 = a_1 + a_2$
A'	ν_4	CH symmetric stretch	$S_4 = r_1 + r_2 + r_3 + r_4$
A'	ν_5	CH symmetric stretch	$S_5 = r_1 - r_2 - r_3 + r_4$
A'	ν_6	CH antisymmetric stretch	$S_6 = r_1 + r_2 - r\,r_3 - r_4$
A'	ν_7	CH antisymmetric stretch	$S_6 = r_1 - r_2 + r_3 - r_4$
A'	ν_8	NH_2/ND_2 scissors	$S_8 = \theta$
A'	ν_9	CC ring stretch	$S_9 = q_3 - q_5 - q_4 + q_6$
A'	ν_{10}	CC ring stretch	$S_{10} = 2q_1 - q_3 - q_5 - 2q_2 + q_4 + q_6$
A'	ν_{11}	CH in-plane deformation	$S_{11} = \alpha_1 - \alpha_2 - \alpha_7 + \alpha_8$
A'	ν_{12}	CH in-plane deformation	$S_{12} = \alpha_3 - \alpha_4 + \alpha_5 - \alpha_6$
A'	ν_{13}	CC ring stretch	$S_{13} = q_1 + q_3 + q_5 - q_2 - q_4 - q_6$
A'	ν_{14}	OH/OD in-plane deformation	$S_{14} = \lambda$
A'	ν_{15}	C—O stretch	$S_{15} = T$
A'	ν_{16}	C—N stretch	$S_{16} = R$
A'	ν_{17}	CH in-plane deformation	$S_{17} = \alpha_1 - \alpha_2 + \alpha_7 - \alpha_8$
A''	ν_{18}	NH_2/ND_2 twist	$S_{18} = \beta_1 - \beta_2$
A'	ν_{19}	CH in-plane deformation	$S_{19} = \alpha_3 - \alpha_4 - \alpha_5 + \alpha_6$
A'	ν_{20}	CC ring stretch	$S_{20} = q_3 - q_5 + q_4 - q_6$
A'	ν_{21}	CC ring stretch	$S_{21} = 2q_1 - q_3 - q_5 + 2q_2 - q_4 - q_6$
A'	ν_{22}	NH_2/ND_2 wag	$S_{22} = \beta_1 + \beta_2$
A''	ν_{23}	CH wag	$S_{23} = \gamma_1 + \gamma_2 - \gamma_3 - \gamma_4$
A'	ν_{24}	CCC in-plane deformation	$S_{24} = \alpha_1 + \alpha_2 - \alpha_7 - \alpha_8$
A''	ν_{25}	CH wag	$S_{25} = \gamma_1 - \gamma_2 + \gamma_3 - \gamma_4$
A''	ν_{26}	CH wag	$S_{26} = \gamma_1 - \gamma_2 - \gamma_3 + \gamma_4$
A'	ν_{27}	CC ring breathing	$S_{27} = q_1 + q_2 + q_3 + q_4 + q_5 + q_6$
A''	ν_{28}	CH wag	$S_{28} = \gamma_1 + \gamma_2 + \gamma_3 + \gamma_4$
A''	ν_{29}	OH/OD torsion	$S_{29} = \eta_1$
A'	ν_{30}	CCC ring in-plane deformation	$S_{30} = \alpha_1 + \alpha_2 + \alpha_7 + \alpha_8$
A'	ν_{31}	CCC ring in-plane deformation	$S_{31} = \alpha_3 + \alpha_4 + \alpha_5 + \alpha_6$
A''	ν_{32}	C – O wag	$S_{32} = \gamma_5$
A'	ν_{33}	CCC ring in-plane deformation	$S_{33} = \alpha_3 + \alpha_4 - \alpha_5 - \alpha_6$
A''	ν_{34}	CCCC ring puckering (τCC)	$S_{34} = 2\tau_1 - \tau_3 - \tau_5 - 2\tau_2 + \tau_4 + \tau_6$
A''	ν_{35}	CCCC ring puckering (τCC)	$S_{35} = \tau_3 - \tau_5 - \tau_4 + \tau_6$
A'	ν_{36}	CCN in-plane deformation	$S_{36} = \rho_1 - \rho_2$
A''	ν_{37}	NH_2/ND_2 torsion	$S_{37} = \eta_2$
A''	ν_{38}	CCCC ring puckering (τCC)	$S_{38} = \tau_3 - \tau_5 + \tau_4 - \tau_6$
A''	ν_{39}	CCCC ring puckering (τCC)	$S_{39} = 2\tau_1 - \tau_3 - \tau_5 + 2\tau_2 - \tau_4 - \tau_6$

[a] Symmetry coordinates are not normalized.

From MP2/6-31G(d), energy differences of 954, 1158 and 847 cm^{-1} have been obtained between **1** and the proposed *gauche* isomers **2**, **7** and **9**, respectively (Figs. 3 and 4). The MP2/6-31G(d) and B3LYP/6-31G(d) predicted frequencies complemented with observed vibrational bands were consistent with either *cis* and/or *trans* conformers (Tables 1, 2 and supplement C). Moreover, *cis* isomer (**1**) is found to be the most stable isomer, but *trans* (**8**) is turned to be more stable upon the addition of diffusion function [21]. Therefore, both *cis* and *trans* isomers are present in solution which is supported by conformer peaks in the OH stretching region [14] along with predicted coincident frequencies presented in Tables 1 and 2. In addition, NCA of high energy *gauche* isomers (**2**, **7** and **9**) and their PEDs are also provided in supplement E. It is noted that the observed wavenumbers for 2AP differs only by ±15 cm^{-1} with those measured for 3AP [14,19].

6.1. OH, NH and CH stretching modes

To isolate the OH and NH_2 fundamentals, we have reproduced MP2 and B3LYP frequencies at 6-31G(d) basis set for $HOC_6H_4NH_2$ and $DOC_6H_4ND_2$ (Tables 1, 2 and supplement C). The NH_2 and/or OH groups are expected to be shifted to lower frequencies in the *deutrated* 2AP. The vibrational assignments of the NH_2/ND_2 and OH/OD stretching modes in 2AP (Tables 1 and 2) were supported by the ratios of $\upsilon_{as}ND_2/\upsilon_{as}NH_2$ (0.75), $\upsilon_sND_2/\upsilon_sNH_2$ (0.73) and υOD/υOH (0.74) in agreement with those reported at ∼0.74, 0.72 and 0.73, respectively, for 3AP [19]. The resolved Raman bands (R_S) observed at 3380 ($\upsilon\upsilon_1$) and 3307 cm^{-1} (υ_3) were assigned to υ_{as} and υ_s NH_2 modes, respectively. The reported NH stretches for 3AP at 3502 and 3418 cm^{-1} [19] are higher than those obtained for 2AP, which reveal stronger hydrogen bonding interaction in 2AP. The calculated N···H distance of 2.048 Å for *cis* conformer

Table 6
Unscaled *ab initio* force field constants (FCs) in mdyne/Å for 2-aminophenol (2AP) and 3-aminophenol (3AP)

Internal coordinates	Symbol	Diagonal force field constants					
		Cis[a] 2AP	*Cis*[b] [16]	*Cis*[c] 3AP	*Trans*[a] 2AP	*Trans*[c] [16]	*Gauche*[a] (9)
$\upsilon(C{-}C)_{av}$	q	6.384	6.429	5.769	6.380	5.769	6.371
$\upsilon C{-}O$	T	6.941	5.48	7.051	6.358	7.051	6.338
$\upsilon O{-}H$	A	7.044		7.884	7.925	7.948	7.928
$\upsilon(C{-}H)_{av}$	r	5.732	5.17	5.448	5.699	5.448	5.704
$\upsilon C{-}N$	R	5.796	5.446	6.348	6.683	5.769	6.610
$\upsilon N{-}H$	a	7.065		7.028	7.321	7.092	7.347
δCCC				1.112		1.112	
δCCO	ε	1.529		1.028	1.486	0.919	1.495
$\delta(CCH)_{av}$	α	1.139	0.439	0.495	1.138	0.495	1.138
δCCN	ρ	1.49		0.723	1.433	0.738	1.434
δCOH	λ	1.041	0.437	0.794	0.836	0.794	0.836
$\delta(CNH)_{av}$	β	0.734	0.491	0.837	0.716	0.837	0.701
δHNH	θ	0.715	0.536	0.502	0.605	0.502	0.604
$\gamma(CH)_{av}$	γ	0.400	0.294	0.297	0.377	0.297	0.383
γCN	γ_6	0.621		0.381	0.621	0.381	0.625
γCO	γ_5	0.750		0.228	0.592	0.228	0.593
$\tau(CCCC)_{av}$	τ	0.193		0.141	0.172	0.137	0.172
$\tau CCOH$	η_1	0.065		0.049	0.010	0.055	0.010
$\tau CCNH$	η_2	0.010		0.053	0.024	0.057	0.015

[a] Calculated *ab initio* FCs at MP_2/6-31G(d) basis set; av: stands for average FCs.
[b] FC's are taken from Ref. [16] which is mainly transferred from Ref. [40].
[c] FC's of 3AP at B3LYP/6-31++G(d,p) basis set are taken from Ref. [19].

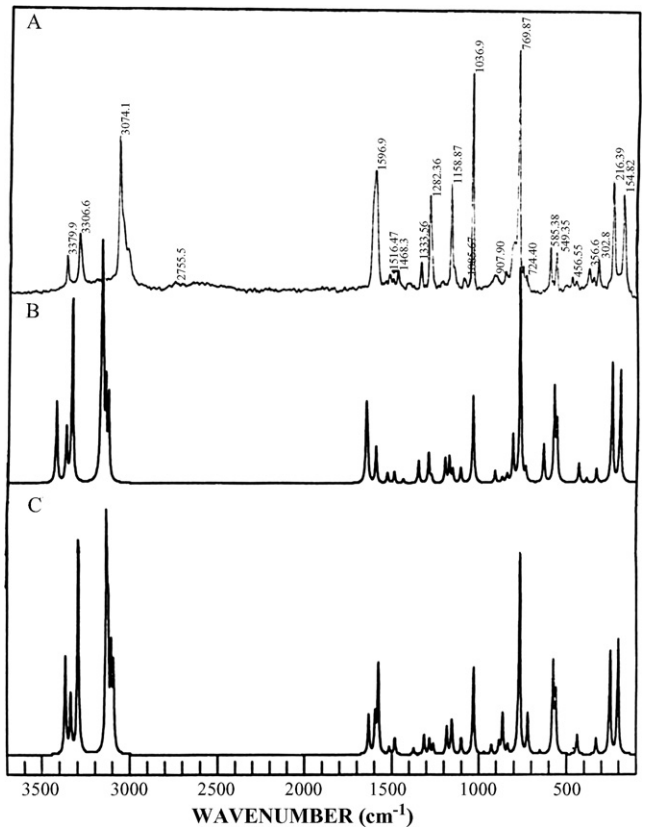

Fig. 6. Raman spectrum of 2-aminophenol; (A) experimental; (B) scaled MP2/6-31G(d) for *cis* isomer; (C) scaled B3LYP/6-31G(d) for *cis* isomer.

is less than ~2.75 Å, the sum of van der Wall radii for nitrogen and hydrogen atoms [56,57], which supports the presence of intramolecular hydrogen bonding in contradiction with Ref. [13]. Moreover, the IR and R spectra of liquid 2AP reveal two split bands for υOH and υOD stretches [14], thus at least *cis* and *trans* isomers are coexist in the liquid phase (Table 1). Similar to N···H, the calculated O···H distance of 2.263 Å for *trans* is less than the sum of van der Wall radii for O and H atoms (~2.72 Å) in favor of intra-molecular hydrogen bonding beside the intermolecular hydrogen bonding [13,55]. As a result, the observed shoulder at 3026 cm^{-1} was assigned to υOH mode. Moreover, the N···H and O···H bond lengths of selected isomers are presented in Figs. 3 and 4 and Table 4. Apparently the hydrogen bonding significance is almost absent in IR spectrum of 2AP (250–4000 cm^{-1}) and 4AP in Nujol cell. The $\upsilon_{as}NH_2$, υ_sNH_2, and υOH fundamentals were assigned to the weak bands at 3450, 3360 and 3295 cm^{-1} in 2AP compared to 3450, 3320 and 3252 cm^{-1} in 4AP, respectively [12]. The observed versus the calculated frequencies (Fig. 6 and supplement D) and vibrational assignments for *cis* and *trans* in solution and *cis* isomer (d_0 and d_3) in the solid phase are listed in Tables 1 and 2.

Owing to the coincident predicted frequencies in the CH stretching region (±9 cm^{-1}, the observed strong polarized bands at 3066 and 3048 cm^{-1} ($R_{Solution}$) are assigned to the four CH stretching modes of *cis* and *trans* isomers (υ_{4-7}). For d_3 isotopomer, the splitted broad at 2000 and 2185 cm^{-1} are the OD stretching mode of *cis* conformer (Table 1). Whereas the observed bands around 2000–1700 cm^{-1} belong to either overtones and/or combination bands.

6.2. Stretching (υCC, υC–N, υC–O) and bending modes below 1600 cm^{-1}

The NH_2 scissors is observed ~1600 cm^{-1} for 2AP [14] and its complexes [16], 3AP [19], *o*-, *m*- and *p*-chloroanilines [11], 2-amino-5-methylphenol [58] and 4-aminosalysilic acid sodium salt [59]. Three overlapped fundamentals separated by ~50 cm^{-1} are expected below 1600 cm^{-1}, they are scaled at 1654 (υ_8), 1647 (υ_9) and 1598 cm^{-1} (υ_{10}). On the other hand, the calculated intensity of NH_2 scissors mode (υ_8) is double that of υCC ring stretches (υ_9 and υ_{10}). Therefore, the centered broad band observed at 1597 cm^{-1} which covers a range of ~100 cm^{-1} in the R_S is chosen mainly for υ_8 ($\delta_{Scissors}$ NH_2) mixed with υ_9 and υ_{10} CC ring stretches (Table 1). According to the calculated frequencies, the observed bands at 1610 (sh) and 1590 cm^{-1} (m) in IR_{Soln} could be assigned for either *cis* or *trans* conformations (Tables 1 and 2). The aforementioned bands match the ring stretching modes υ_9 and υ_{10} of *cis* isomer, respectively but they are altered for the *trans* isomer. Moreover, the experimental depolarization measurements had faced difficulties [14] which perhaps enlighten the hesitant dp Raman band at 1592 cm^{-1}, this band must belong to A' species.

The calculated FC's of υCO and υCN are 6.941 and 5.796 mdyne/Å, respectively. Therefore the C–O (υ_{15}) and C–N (υ_{16}) stretches are coupled together as seen in the PEDs Tables 1 and 2. Thus υ_{15} and υ_{16} are assigned to the observed bands at 1282 cm^{-1} (vs) and 1265 cm^{-1} (vw), in agreement to mixed vibrational modes of υ_S NCCO and υ_{as} NCCO [14], respectively. On the other hand, υ_{15} and υ_{16} for *cis* and *trans* isomers are separated only by ~20–40 cm^{-1} (Table 1), these bands could be assigned for either *cis* and *trans* conformers.

The IR band reported at 1228 cm^{-1} (1220 vw in R_S) is confidently assigned to δ_{ip}CH (υ_{17}). And the two fundamentals scaled at 1178/1159 cm^{-1} are devoted to υ_{19}(p)/υ_{18}(dp), where the CH in-plane bending (υ_{19}) match the observed polarized band at 1154 cm^{-1} (R_{Soln}). Otherwise, non of δ_{ip}CHs are expected below 1150 cm^{-1} accordingly, the observed bands 1122/1159 cm^{-1} in R_{Soln}/R_S spectra are favorably consistent with $\delta_{twist}NH_2$ (υ_{18}) [58,59] rather than δ_{ip}CH [12,14], see Tables 1 and 2.

Four intensively mixed ring stretches (υCC) are remaining, υ_{13} and υ_{20} are observed at 1410 and 1086 cm^{-1}, respectively. And υ_{21} and υ_{27} (ring breathing) are consistent with those observed at 1037 and 770 cm^{-1}, respectively (Table 1). The foregoing fundamental is 43% ring breathing mode (υ_{27}) mixed with υCN (υ_{16}) and υCO (υ_{15}) which deviates little bit with those observed at 810 and 768 cm^{-1} [14,58]. For d_3 2AP, the observed bands at 748/753 cm^{-1} in the IR_S/R_S scaled at 774/721 cm^{-1} could be interpreted for υ_{27}/υ_{22} (ring breathing/ND_2 wag) of *cis* conformer. The observed IR bands at 1080/1024 cm^{-1} scaled at 1113/1043 cm^{-1} are assigned to υ_{20} and υ_{21} ring stretches for 2AP (d_0), respectively. These fundamentals (υ_{20} and υ_{21}) are scaled at 1129 and 1046 cm^{-1} for the deutrated isotopmer (Table 1). On contrary, these bands (1080 and 1024 cm^{-1}) were inaccurately assigned to NH_2 and CH bending modes, respectively [12,14]. For 2AP and 3AP, the υC=C ring stretches were observed in the region of ~1605–1300 cm^{-1} along with an extra band ~1000 cm^{-1} or 860 cm^{-1} [12,14,19] in agreement with our theoretical predictions except for δ_{ip}CH (υ_{11}). The δ_{ip} CH (υ_{11}) properly fits the observed weak band at 1516 cm^{-1} in the R_S regardless of the minor features of υ_{20} and υ_{21} as expressed in the PEDs. Moreover, the broad band at 1468 cm^{-1} scaled at 1493 cm^{-1} is assigned to δ_{ip}CH (υ_{12}). Additionally, δ_{ip}OH (υ_{14}) is obviously mixed with an overtone which was imprecisely assigned to the observed band at 1410 cm^{-1} [14]. Nevertheless, this band is probably υCC ring stretch (υ_{13}) rather than the suggested δ_{ip}OH. Moreover, the weak band at 1334/1397 cm^{-1} (R_S/unscaled) is assigned to δ_{ip}OH (υ_{14}) which is shifted to 1009 cm^{-1} for δ_{ip}OD at the same level (Table 1).

As a result of current NCA several fundamentals of *cis* and *trans* isomers are strongly deviated whereas the dp ratios were incomplete due to experimental obstacles [14]. Thus we have focused on the estimated MP2 frequencies for vibrational modes below 1000 cm^{-1} regardless of their coincidences, Tables 1 and 2. The calculated NH_2 wagging frequency is exceedingly dependent on the levels of calculations. For instance, the NH_2 wagging mode (υ_{22}) scaled at 918/707 cm^{-1} for *cis*/*trans* isomers. From MP2/6-31G(d) frequency calculations, none of *trans* fundamentals are estimated around 900 cm^{-1}, accordingly the observed weak band at 925/924 cm^{-1} (IR_{Soln}/IR_S) should belong to *cis* conformer (υ_{22}). However, wavenumbers ~900 cm^{-1} are calculated for both *cis* and *trans* isomer utilizing B3LYP level at the same basis set.

The assignments of the observed IR bands at 897 (υ_{24}), 869 (υ_{23}), 846 (υ_{25}), 766 (υ_{27}) and 747 (υ_{28}) cm^{-1} [14] are consistent with calculated wavenumbers and PED's (Tables 1 and 2). However, vw IR intensities (0.068) and Raman activities (0.7) are predicted for δCH wagging mode (υ_{23}), therefore the observed vw Raman band at 887 cm^{-1} is assigned for υ_{23} for the -d_3 isomer. Aided by NCA, the $\delta_{wag}NH_2$ (υ_{22}) and δ_{wag}CH (υ_{26}), are assigned for the observed bands at 924, and 802 cm^{-1}, respectively which disagree with Ref. [14].

The observed very weak bands at 582 (1, p), 569 (w) cm^{-1} in R_{Soln} spectrum are assigned to δ_{ccc} ring bending mode in harmony with Refs. [12,14]. On the other hand, the polarized vw band at 546 cm^{-1} is inaccurately assigned to the A'' ring torsion, however it fits and dominates the C–O wagging mode (υ_{32}) with minor features of ring puckering modes (10–13% of υ_{34} and υ_{35}). There is an extra weak band observed at 487 cm^{-1} could be claimed to the OH torsion (uscaled/scaled at 734/550 cm^{-1}) which is comparative to 439 cm^{-1} for peroxynitrous acid (HOONO) as reported by McCoy et al. [60].

Due to the lack of computational calculation [12,14] most of the vibrational modes below 500 cm^{-1} are reassigned herein. The reported band at 333 and 437 cm^{-1} are properly harmonize the higher contributions of δCCN (υ_{36}), δCCC (υ_{33}) and τCC (υ_{34}) scaled at 334, 436 and 432 cm^{-1}, respectively (Table 1).

The region below 400 cm^{-1} could possibly have either υN···H, υO···H, τNH_2 and ring puckering mode(s) [59,61,62]. At the levels of B3LYP and MP2, large difference of ~260 cm^{-1} has been calculated for ring puckering fundamental (υ_{35}). The fundamental amino torsions have been observed at 275 and 228 cm^{-1} for CH_2=$CHCH_2NH_2$ which shift to 209

and 171 cm^{-1}, respectively [63] for ND_2. Furthermore, the τNH_2 was observed at 280 cm^{-1} (IR_{gas} and R_{Soln}) for 1,1-dimethylhydrazine [44]. Therefore, the observed vw band at 279 cm^{-1} (R_S) could be assigned to NH_2 torsion (shifted to 300 cm^{-1} in R_{Soln}), see Table 1. Whereas, the recorded band at 217 cm^{-1} (R_S) definitely represents the light contribution ring puckering (υ_{38}). On the other hand υ_{39} is beyond our spectral measurements.

The OH torsion potential functions for the hindered internal rotation of the O···H and O···D groups were evaluated in the region of 286–283 cm^{-1} [61]. For ethanol, the O···H torsion is observed at 202.6 and at 243.1 cm^{-1} for *trans* and *gauche* conformers, respectively. An asymmetric potential function utilizing these transitions gives an average value of 401 cm^{-1} [62]. Therefore, the unassigned strong Raman band at 155(6) cm^{-1} [14] is chosen for the O···H fundamental (Fig. 1) in favor of intramolecular hydrogen bonding compared to 165 cm^{-1} in the R_{Soln} spectrum of 4-aminosalicylic acid [59].

7. Barriers to internal rotation

7.1. NH_2 Barriers to internal rotation

To obtain NH_2 barriers to internal rotation, the NH_2 moiety was rotating around C–N bond by 10° increments while the OH group is fixed either towards **1** or away **6** from NH_2 group. Potential surface scans (PSS) were carried out for the aforementioned conformers using optimized SPs from MP_2/6-31G(d) basis set. The detailed results of the predicted barriers to internal rotations are summarized in supplement F.

The **1** (*cis*) to **2** NH_2 barrier (supplement F) is estimated to be 1418 cm^{-1} (16.9 kJ/mol ≡ 4.02 kcal/mol), however only ~31 cm^{-1} is predicted for the barrier between **1** (*cis*) and **3** conformers (where the nitrogen lone pair is out of plane by 10°). This very low barrier is probably the incentive for the conversion of **3** to be more likely the stable **1** (*cis*) configuration (3→1). On the other hand, very high barriers of 6431 (18.2 kcal/mol) and 3428 cm^{-1} (9.7 kcal/mol) were obtained for **1** (*cis*) to **4** and **5** compared to energy differences (ΔE) of 2688 (7.6 kcal/mol) and 2089 cm^{-1} (5.9 kcal/mol) achieved from MP2/6-31G(d), respectively. These values along with the calculated imaginary frequencies ensure that **4** and **5** conformers are transition states. It is worth mentioning that, high NH_2 barriers were predicted around 11-12 kcal mol^{-1} for formamidine, HC(=NH)NH_2 and acetamidine, CH_3C(=NH)NH_2 by semi empirical and *ab initio* calculations with the minimal, double-zeta, polarized double-zeta basis sets [64]. On the other hand, relatively low NH_2 barriers were obtained, $V_1 = 279 \pm 16$ (0.79 ± 0.04 kcal/mol) and $V_3 = 707 \pm 4$ cm^{-1} (2.03 ± 0.01 kcal/mol) for $CH_3CH_2NH_2$ [65] by means of Raman spectroscopy. Moreover, the NH_2 inversion barrier was estimated at 0.5 and 1.6 kcal/mol for vinylamine (CH_2=CH–NH_2) and 2.3 and 3.3 kcal/mol for keteneamine (O=C=CH–NH_2) at B3LYP/6-311+G(d,p) and MP2/6-311+G(d,p) levels [66], compared to 1.0 kcal/mol (356 cm^{-1}) for vinylamine from its microwave spectrum. These differences in NH_2 barriers are devoted to either weak or strong hydrogen bonding interactions.

Low NH_2 barriers of 228 (646 cal/mol) and 674 cm^{-1} (1.9 kcal/mol) are calculated between **8** (*trans*) and other *gauche* forms **7** and **9** (supplement F), respectively. Therefore we could not ignore **9** (*gauche*) completely throughout the current study due to lack of experimental facilities at low- and high-temperatures. Moreover, these relatively low barriers may account for the analogous in calculated frequencies for **7**, **8** and **9** *gauche* conformers and their PEDs (supplement E). Likewise, the deviations in the predicted wavenumber are ±10 cm^{-1} below 3300 cm^{-1} and ~50–70 cm^{-1} for OH and NH_2 stretching modes. Therefore, we have focused basically on **1** (*cis*) and **8** (*trans*) throughout this manuscript.

7.2. OH Barriers to internal rotation

The OH group of **1** (*cis*) conformer was rotated by 10° increments around C–O bond while the NH_2 group is fixed (supplement F). At the beginning the energy of **1** is −361.6866096 Hartree and the rotation of OH by 10° increments cause an energy increase till reaching a maximum (τHOCC = 90°) at conformer **11** (E = −361.66378 Hartree) which is called *perpendicular* configuration (i.e. OH is ⊥ to benzene ring). Further increase of $\tau > 90°$ reveals gradual decrease till reaching conformer **6**, producing high OH barrier of 14.2 kcal/mol (5011 cm^{-1}) between **11** and **1** isomers. And the **6** to **1** OH barrier is found to be 10.5 kcal/mol (3723 cm^{-1}). Moreover, OH barrier of 3.6 kcal/mol (1288 cm^{-1}) is obtained between **6** and **11** rotamers (supplement F). The preceding value is consistent with V_2 barriers of 1213 and 1007 cm^{-1} obtained from the far-IR spectrum of gaseous phenol and *p*-fluorophenol, respectively [67]. Moreover, V_{OH} was calculated in the range of 2.0 kcal/mol (707.5 cm^{-1}) to 2.3 kcal/mol (804.9 cm^{-1}) utilizing MP4(SDQ)/cc-pVTZ *ab initio* calculations of 2,2,2-trifluoroethanol [61]. These aforesaid high OH barriers as well as the calculated imaginary frequencies unquestionably allow the exclusion of **6** and **11** isomers.

8. Force constants in internal coordinates

The MP2/631G(d) *ab initio* FCs in internal coordinates for **1** (*cis*), **8** (*trans*) isomers and **2** as an example for the *gauche* isomers (**2**, **7** and **9**) are summarized in Table 6. Most of the FCs for the two conformers differs by less than 3%(the average FCs of C=C's, C–H's and CCH's) but there are some notable exceptions. FCs deviations of ~12% for υOH and τCCCC, ~14% for CH wagging and 17% for CCCC ring torsions have been observed. Moreover, considerable changes of ~26, ~25, ~22, ~18 and 15% were obtained for γCO, δCOH, τCCNH, δHNH and γCN FCs, respectively. Furthermore, the FC's of 2AP and 3AP [19] experience minor changes for stretching vibrational modes, which is not the case for the bending fundamentals (Table 6). It is worth mentioning that, the reported FCs for 2AP and its complexes [16] was mainly transferred from that of nitrobenzene [40]. The transferred stretching FCs agrees within ±10%, but the bending FC's are ~40% lower than our values. In addition we could not correlate all current FCs due to lack of

internal coordinate notifications [16], definitely the calculated FCs herein are considered better than those represented earlier [16].

9. Structural parameters

The calculated bond distances and the CCC angles from B3LYP (supplement A) and MP2 (Table 3) levels for *cis* and *trans* isomers does not differ significantly. Moreover, the SPs agree well with x-ray values within the experimental errors [25] as well as those calculated from combined B3LYP/6-311+G(2d,2p)//B3LYP/6-31G(d) method [21]. The C–O and C–N bond length vary only by 0.01–0.001 Å and the NCC angle varies by ±0.1° at MP2 and B3LYP levels at the same basis set. And the calculated angles were frequently consistent with X-ray values [25] by ±2–5° (e.g., $\angle N_4C_3C_5$, $\angle O_2C_1C_{11}$ and $\angle C_1C_{11}H_{12}$), ±1–2° (e.g., $\angle C_9C_7H_9$, $\angle C_{11}C_9H_{10}$) and less than 1° in other cases as in CCC angles, see Table 3.

From x-ray study of 2AP [25], it was already established that the benzene ring is not completely planar, it is little bit tilted by 0.007 Å. Therefore, both the angular distortion of the benzene ring and the electronegativity of the subsistent groups are expected to affect the CCC internal angles [68]. The angles of $C_1C_3C_5$ (C_3 attached to nitrogen atom) and $C_3C_1C_{11}$ (C_1 attached to oxygen atom) are determined to be 120.5(5)° and 119.6(5)°, respectively. Moreover, from electron diffraction (ED) study for *p*-bromonitrobenzene, the $\angle CCC_{Br}$ and $\angle CCC_N$ are determined to be 122.6(2)° and 121.6(2)°, respectively [68]. Accordingly, the attachment of benzene ring to less electronegative atom causes an increase of ∠CCC angle compared to that attached to more electronegative atom. However, the *ab initio* predictions for $\angle C_1C_3C_5$ and $\angle C_3C_1C_{11}$ are opposite to the experimental values. The presence of intramolecular hydrogen bonding causes decreasing of $\angle N_4C_3C_1$ and $\angle O_2C_1C_3$ accompanied by simultaneous increase of $\angle N_4C_3C_5$ and $\angle O_2C_1C_{11}$, respectively see Table 4. The calculated torsion angles of $C_1C_3N_4H_{14}$ and $C_1C_3N_4H_{15}$ from MP2 level is larger than those predicted from B3LYP by ∼1–3°.

10. Conclusion

RHF, B3LYP and MP2 computational results for 2-aminophenol (2AP) are consistent with *cis* (OH is directed towards NH_2) and *trans* (OH is away from the NH_2 moiety and the NH bonds and nitrogen lone-pair are out-of-plane) conformers in solution and more likely *cis* isomer in the solid phase. *Ab initio* and DFT calculations were in favor of *cis* conformer to be the most stable except RHF/6-31++G(d,p) was in favor of *trans*. These calculations do not provide absolute differences between *cis* and *trans* isomers. Revised vibrational assignments for *cis* and *trans* 2AP has been proposed and supported by calculated frequencies combined with normal coordinate analysis and potential energy distributions. Moreover, the NH_2 and OH barriers to internal rotations, allow the prospect of extra three *gauche* structures.

Acknowledgements

TAM sincerely thanks Professor James R. Durig, Molecular Spectroscopy Laboratory, Chemistry Department, University of Missouri-Kansas City, MO64110, USA, for giving him the opportunity to use G- and F-matrix programs to calculate FCs in internal coordinates and PEDs. The authors appreciate the free access to the IR spectrum of 2-aminophenol by the National Institute of Advanced Industrial Science and Technology (AIST), Japan (http://www.aist.go.jp/RIODB/SDBS).

Appendix A. Supplementary data

Supplementary data associated with this article can be found, in the online version, at doi:10.1016/j.saa.2006.12.047.

References

[1] H. Yang, A.J. Bard, J. Electroanal. Chem. 339 (1992) 423.
[2] N. Yamada, K. Teshima, N. Kobayashi, R. Hirohashi, J. Electroanal. Chem. 394 (1995) 71.
[3] R. Lapuente, F. Cases, P. Garcés, E. Morallón, J.L. Vázquez, J. Electroanal. Chem. 451 (1998) 163.
[4] L.Y. Wang, L. Wang, C.Q. Zhu, J.L. Liu, L. Li, J.K. Yao, Anal. Lett. 35 (2002) 2259.
[5] L. Hanysova, P. Kastner, J. Klimes, Chem. Listy 98 (2004) 152.
[6] S. Kunimra, T. Ohsaka, N. Oyama, Macromolecules 21 (1988) 894.
[7] C. Barbero, J.J. Silber, L. Sereno, J. Electroanal. Chem. 291 (1990) 81.
[8] R. Huang, H. Okuno, M. Takasu, S. Takeda, H. Kano, Y. Shiozaki, K. Inoue, Jpn. J. Pharmacol. 83 (2000) 182.
[9] J.C. Evans, Spectrochim. Acta 16 (1960) 428.
[10] R.J. Jackobsen, E.J. Brewer, Appl. Spectrosc. 16 (1962) 32.
[11] V.B. Singh, R.N. Singh, I.S. Singh, Spectrochim. Acta 22 (1966) 927.
[12] V.N. Verma, D.K. Rai, Appl. Spectrosc. 24 (1970) 445.
[13] P.J. Krueger, Tetrahedron 26 (1970) 4753.
[14] W.P. Griffith, T.Y. Koh, Spectrochim. Acta 51A (1995) 253.
[15] O. Paulsen, Monastsh Chem. 72 (1939) 244.
[16] K. Bahgat, A.S. Orabi, Polyhedron 21 (2002) 987.
[17] M. Baia, F. Toderas, L. Baia, J. Popp, S. Astilean, Chem. Phys. Lett. 422 (2006) 127.
[18] K. Jackowska, J. Bukowska, A. Kudelski, J. Electroanal. Chem. 350 (1993) 177.
[19] Y. Buyukmurat, S. Akyuz, J. Mol. Struct. 744–747 (2005) 921.
[20] M.A. Palafox, M. Gill, J.L. Núñez, Vibr. Spectrosc. 6 (1993) 95.
[21] J.R.B. Gomes, M.A.V. Da Silva, Int. J. Quantum Chem. 101 (2005) 860.
[22] Y. Xie, H. Su, W.B. Tzeng, Chem. Phys. Lett. 394 (2004) 182.
[23] C. Unterberg, A. Gerlach, A. Jansen, M. Gerhards, Chem. Phys. 304 (2004) 237.
[24] H. Mori, H. Kugisaki, Y. Inokuchi, N. Nishi, E. Miyoshi, K. Sakota, K. Ohashi, H. Sekiya, Chem. Phys. 277 (2002) 105.
[25] S. Ashfaquzzaman, A.K. Pant, Acta Cryst. 35B (1979) 1394.
[26] M.J. Frisch, G.W. Trucks, H.B. Schlegel, G.E. Scuseria, M.A. Robb, J.R. Cheeseman, V.G. Zakrzewski, J.A. Montgomery Jr., R.E. Stratmann, J.C. Burant, S. Dapprich, J.M. Millam, A.D. Daniels, K.N. Kudin, M.C. Strain, O. Farkas, J. Tomasi, V. Barone, M. Cossi, R. Cammi, B. Mennucci, C. Pomelli, C. Adamo, S. Clifford, J. Ochterski, G.A. Petersson, P.Y. Ayala, Q. Cui, K. Morokuma, D.K. Malick, A.D. Rabuck, K. Raghavachari, J.B. Foresman, J. Cioslowski, J.V. Ortiz, A.G. Baboul, B.B. Stefanov, G. Liu, A. Liashenko, P. Piskorz, I. Komaromi, R. Gomperts, R.L. Martin, D.J. Fox, T. Keith, M.A. Al-Laham, C.Y. Peng, A. Nanayakkara, C. Gonzalez, M. Challacombe, P.M.W. Gill, B. Johnson, W. Chen, M.W. Wong, J.L. Andres, C. Gonzalez, M. Head-Gordon, E.S. Replogle, J.A. Pople, Gaussian 98, Revision A.7, Gaussian, Inc., Pittsburgh, PA, 1998.
[27] W.J. Hehre, L. Radom, P.V.R. Schleyer, J.A. Pople, *Ab initio* Molecular Orbital Theory, Wiley, NY, 1986.

[28] C.E. Dykstra, *Ab intio* Calculations for the Structures and Properties of Molecules, Elsevier Science Publishing Co. Inc., NY, 1988.
[29] C. Moller, M.S. Plesset, Phys. Rev. 46 (1934) 618.
[30] A.D. Becke, Phys. Rev. 38A (1988) 3098.
[31] C. Lee, W. Yang, R.G. Parr, Phys. Rev. 37B (1988) 785.
[32] A.D. Becke, J. Chem. Phys. 98 (1993) 5648.
[33] D.C. Young, Computational Chemistry, John Wiley and Sons Inc., 2002 (Chapter 5).
[34] J.J.P. Stewart, J. Comp. Chem. 10 (1989) 221.
[35] Quantum CAChe 3.2 User Guide, Oxford Molecular Ltd., 1999 (Chapter 18).
[36] P. Pulay, Mol. Phys. 17 (1969) 197.
[37] S. Portmann, H.P. Lüthi, Chimia 54 (2000) 766.
[38] F.A. Cotton, Chemical Applications of Group Theory, 2nd ed., John Wiley & Sons, 1971.
[39] E.B. Wilson, J.C. Decius, P.C. Cross, Molecular Vibrations, McGraw Hill, NY, 1955 (republished by Dover: New York, 1980).
[40] A. Kuwae, K. Machida, Spectrochim. Acta 35A (1979) 27.
[41] H.J. Schachtshneider, Vibrational Analysis of Polyatomic Molecules, Parts V and VI, Technical Reports Nos. 231and 57, Shell Development Co., Houston, TX, 1964/1965.
[42] Y. Yamauchi, M. Frisch, J. Gaw, H.F. Schaefer III, J. Chem. Phys. 84 (1986) 2262.
[43] G.M. Kuramshina, F. Weinhold, J. Mol. Struct. 410–411 (1997) 457.
[44] J.R. Durig, C. Zheng, J. Mol. Struct. 690 (2004) 31.
[45] P. Pulay, X. Zhou, G. Fogarasi, in: R. Fausto (Ed.), Recent Experimental and Computational Advances in Molecular Spectroscopy, Kluwer Academic Publishers, The Netherlands, 1993, p. 99.
[46] M.A. Palafox, V.K. Rastogi, Spectrochim. Acta 58A (2000) 411.
[47] T.A. Mohamed, J. Mol. Struct. Theochem. 713 (2005) 179.
[48] T.A. Mohamed, M.M. Abo Aly, J. Raman Spectrosc. 35 (2004) 869.
[49] J.R. Durig, G.A. Guirgis, C. Zheng, T.A. Mohamed, Spectrochim. Acta 29A (2003) 2099.
[50] G.W. Chantry, in: A. Anderson (Ed.), Raman Effect, vol. 1, Marcel Dekker Inc., NY, 1971 (Chapter 2).
[51] M.J. Frisch, Y. Yamaguchi, J.F. Gaw, H.F. Schaefer, J.S. Binkley, J. Chem. Phys. 84 (1986) 531.
[52] R.D. Amos, Chem. Phys. Lett. 124 (1986) 376.
[53] P.L. Polavarapu, J. Phys. Chem. 94 (1990) 8106.
[54] T.A. Mohamed, G.A. Guirgis, Y.E. Nashed, J.R. Durig, Vibr. Spectrosc. 30 (2002) 111.
[55] J.G. David, H.S. Hallam, Spectrochim. Acta 21 (1965) 841.
[56] A. Bondi, J. Phys. Chem. 68 (1964) 441.
[57] J.E. Huheey, E.A. Keiter, R.L. Keiter, Inorganic Chemistry: Principles of Structure and Reactivity, 4th ed., Harper Collins, NY, USA, 1993.
[58] N. Sundaraganesan, B. Anand, B.D. Joshua, Spectrochim. Acta Part A 67 (2007) 550.
[59] C.Y. Panicker, H.T. Varghese, A. John, D. Philip, K. Istvan, G. Keresztury, Spectrochim. Acta 58A (2002) 281.
[60] A.B. McCoy, J.L. Fry, J.L. Francisco, A.K. Mollner, M. Okumura, J. Chem. Phys. 122 (2005) 104311.
[61] M.L. Senent, A. Perez-Ortega, A. Arroyo, R. Domínguez-Gómez, Chem. Phys. 266 (2001) 19.
[62] J.R. Durig, R.A. Larsen, J. Mol. Struct. 238 (1990) 195.
[63] J.R. Durig, J.F. Sullivan, C.M. Whang, Spectrochim. Acta 41A (1985) 129.
[64] W. Kinasiewicz, A. Les, I. Wawer, J. Mol. Struct. Theochem. 168 (1988) 1.
[65] J.R. Durig, Y.S. Li, J. Chem. Phys. 63 (1975) 4110.
[66] H.M. Badawi, J. Mol. Struct. Theochem. 726 (2005) 253.
[67] N.W. Larsen, F.M. Nicolaisen, J. Mol. Struct. 22 (1979) 29.
[68] A. Almenningen, J. Brunvoll, M.V. Popik, L.V. Vilkov, S. Samdal, J. Mol. Struct. 118 (1984) 37.